Realistic modeling of the electronic structure and the effect of correlations for Sn/Si(111) and Sn/Ge(111) surfaces

Sergej Schuwalow, Daniel Grieger, and Frank Lechermann
I. Institut für Theoretische Physik, Universität Hamburg, D-20355 Hamburg, Germany
(Received 16 March 2010; published 19 July 2010)

The correlated electronic structure of the submonolayer surface systems Sn/Si(111) and Sn/Ge(111) is investigated by density-functional theory and its combination with explicit many-body methods. Namely, the dynamical mean-field theory and the slave-boson mean-field theory are utilized for the study of the intriguing interplay between structure, bonding, and electronic correlation. In this respect, explicit low-energy one- and four(sp^2-like)-band models are derived using maximally localized Wannier(-type) functions. In view of the possible low-dimensional magnetism in the Sn submonolayers we compare different types of magnetic orders and indeed find a 120° noncollinear ordering to be stable in the ground state. With single-site methods and cellular-cluster extensions the influence of a finite Hubbard U on the surface states in a planar and a reconstructed structural geometry is furthermore elaborated.

DOI: 10.1103/PhysRevB.82.035116 PACS number(s): 71.15.Mb, 73.20.At, 71.10.Fd, 71.30.+h

I. INTRODUCTION

Strong electronic correlations lead to many of the most interesting phenomena in modern condensed-matter physics, such as superconductivity, the metal-insulator transition, or local-moment magnetism. It is well known that the influence of these many-body effects depends heavily on the interplay between structure, bonding, and the degree of order within the effective dimensionality of the given problem. While the study of realistic bulk systems in this context has been rather extensive in recent years, those investigations may only provide insight into the effect of dimensionality via reasonably justified quasidimensions due to large crystalline anisotropies. In this respect the study of surface systems has the advantage that by an intelligible tuning of the coupling between the adsorbate and the substrate, quasi-low-dimensionality can be created more efficiently. Besides, there are many surface-sensitive experimental probe techniques in order to reveal the electronic structure more directly than in the bulk. Hence the research on specific surface materials problems may add substantially to the understanding of the general problem of strong quantum correlations.

There has been an increased interest in adsorbate systems involving semiconducting substrates since more than a decade.[1–3] These often exhibit dangling-bond-derived surface states with rather small bandwidths. While Mott criticality is hardly seen on the free surfaces because of structural reconstructions, certain adsorbate atoms forming (sub)monolayers stabilize hybridized narrow-band surface states down to low temperatures. The most prominent of this kind are the so-called α-phase surfaces[1] where the canonical structure is described by a $\sqrt{3}\times\sqrt{3}R30°$ triangular array of adsorbate atoms within a 1/3 monolayer coverage on a (111) semiconductor substrate, resulting in a half-filled surface band. Due to the rather large interatomic distances between the adsorbate atoms (~7 Å) the latter becomes indeed rather narrow. Mott-insulating phases in such systems are believed to be realized in, e.g., K/Si(111) (Ref. 2) whereas a transition to a correlation-driven charge-density-wave phase takes place in Pb/Ge(111).[1]

In this respect, the α-phase systems Sn/Si(111) and Sn/Ge(111) (Fig. 1) are of central interest due to the unusual properties they exhibit at low temperatures. It has been recently verified by Modesti *et al.*[4] that the planar α-Sn/Si(111) surface exhibits a metal-insulator transition below 60 K. No structural reconstruction appears to accompany this transition since it was observed[5] that the $\sqrt{3}\times\sqrt{3}R30°$ periodicity is stable at least down to around 6 K. The question of magnetic ordering within the insulating regime, i.e., the formation of an antiferromagnetic (AFM) Mott-insulating state, has been raised because of band foldings revealed by low-T photoemission experiments[4,6,7] leading to a 3×3 periodicity. In contrast, the structurally and electronically very similar α-Sn/Ge(111) surface shows vastly different behavior. There a transition from the $\sqrt{3}\times\sqrt{3}R30°$ phase at room temperature to a 3×3 symmetry below 200 K takes place. Two competing ground-state configurations of the Sn atoms seem to exist in the latter temperature range,[8] with the so-called two-down-one-up (2D-1U) (i.e., two Sn atoms down, one Sn atom up with respect to the planar-triangular structure) state in favor of 6 meV/adatom against the competing one-down-two-up

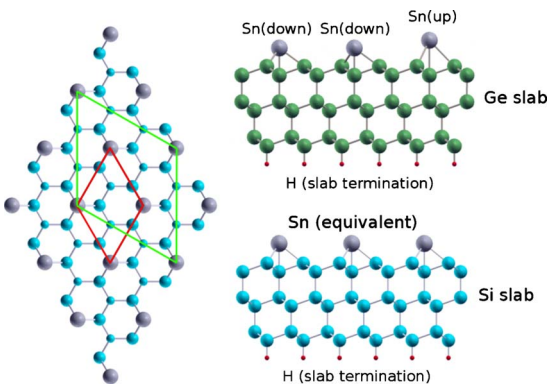

FIG. 1. (Color online) Left: top view onto the employed $\sqrt{3}\times\sqrt{3}R30°$ (red/dark gray) and 3×3 (green/light gray) surface unit cells. Right: side view of the slab geometry for the Sn/Si(111) surface (bottom) and the distorted 1U-2D Sn/Ge(111) surface (top).

configuration.[9] The $\sqrt{3}\times\sqrt{3}R30°$ periodicity observed at room temperature is understood as a result of the rapid fluctuations of the system between these two states.[8] It is still a matter of debate whether or not the system displays a surface Mott transition similar to the Sn/Si(111) system. The finding of a Mott-insulating phase in α-Sn/Ge(111) below 20 K by Cortés *et al.*[10] has apparently not been confirmed by other groups.[11,12]

The electronic structure of the α surface phases poses an interesting problem in the context of strong electron correlation. Early phase-diagram studies of such adlayer structures within the Hartree-Fock approximation showed the possibility for various orderings.[13] Since the narrow-band surface state is mainly derived from a hybridization of the Sn($5p_z$) state with the underlying Si states, one deals with Coulomb correlations in an effective $5p$ system (assuming a local Hubbard-type interaction). Calculations based on standard density-functional theory (DFT) show[14,15] in the case of $\sqrt{3}\times\sqrt{3}R30°$ Sn/Si(111) indeed an isolated half-filled surface band of width $W\sim 0.3$ eV. Additionally, the named 3×3 reconstruction in Sn/Ge(111) is verified within DFT.[8,9,16–19] Correlation effects beyond the local-density approximation (LDA) and the generalized-gradient approximation (GGA) have been investigated by Profeta and Tosatti[20] within the LDA+U method,[21] establishing a Hubbard U for the single Sn($5p_z$) orbital. In this scheme, Mott-insulating Sn/Si(111) (with assuming ferromagnetic/ferrimagnetic order) is reached for $U\simeq 2$ eV but the authors find a $U\simeq 4$ eV from constrained calculations more appropriate, also to cope with a gap size of order ~ 0.3 eV. This rather large value for the local Coulomb interaction differs from $U_{\mathrm{eff}}\simeq 1.15$ eV obtained in elder constrained LDA calculations designed for a minimal model describing the surface band.[15] Concerning α-Sn/Si(111) there are speculations[4,13,20] about a realization of the quasi-two-dimensional (2D) correlated triangular lattice problem, including the possibility of antiferromagnetism or spin-liquid physics and d-wave superconductivity.

In this work we want to investigate the importance of electronic correlations and their interplay with the structural data in the α-Sn/(Si,Ge)(111) phases. By means of a combination of realistic DFT band-structure schemes with advanced many-body techniques, the aim is to clarify the differences stemming from the (Si,Ge)(111) substrates and to reveal to which extent Coulomb correlations can give rise to the observed and perhaps still-to-be observed phenomena. Albeit some relevant work has already been performed in this direction, namely, Refs. 13, 15, and 20, there remain still many open questions. For instance, the minimal Hubbard model derived by Flores *et al.*[15] has not truly been numerically treated and the arguments given concerning the influence of structural reconstructions on a possible Mott criticality lack a local picture of the involved orbitals. The LDA+U method utilized in Ref. 20 is designed for long-range-ordered insulating states and neglects as a static technique quantum fluctuations (even in the Mott state). Hence correlations in the metallic regime are usually described incorrectly and magnetic tendencies are often overestimated. Moreover, the experimental data is far from being conclusive, e.g., concerning the appearance of local-moment physics and eventual magnetic ordering.

II. THEORETICAL APPROACH

Realistic theoretical schemes for correlated condensed matter, combining traditional band-structure approaches with explicit many-body techniques have been quite successful in the last decade in dealing with various problems in strongly correlated physics. The most prominent of such schemes is the combination of DFT with the dynamical mean-field theory (DMFT), the so-called LDA+DMFT (Refs. 22 and 23) framework. While in standard DFT correlation effects are only taken into account in an averaged way by making reference to a homogeneous(like) electron gas, the named combined approach allows for explicit many-body effects on an operator level by still keeping important band-structure details from LDA. The DMFT technique[24,25] is able to incorporate all onsite quantum fluctuations and thereby may describe quasiparticle (QP) as well as atomic excitations (i.e., Hubbard bands) on an equal footing. A alternative combined approach is given by interfacing the Gutzwiller or the slave-boson mean-field technique with DFT.[26–28] In this more simplified treatment the QP lifetime remains infinite, thus omitting the full frequency dependence of the self-energy. Hence only low-energy features may be addressed in the spectral function and hence high-energy Hubbard bands are not accessible. However, importantly, the local-atomic multiplets are still present with an effective static character in the generalized theory.[29–31]

Due to the subtle dependencies of the α-Sn/(Si,Ge)(111) surface electronic structure on the structural facts, care must be taken in its proper determination. We used an implementation[32] of the highly accurate mixed-basis pseudopotential (MBPP) technique[33] for this task. This DFT band-structure code employs norm-conserving pseudopotentials[34] and an efficient combined basis consisting of plane waves and a few localized orbitals. Since the magnetism of these surface systems is very subtle, we additionally performed computations within the projector-augmented-wave (PAW) method[35] for the specific study of magnetic ordering. Thereby one is able to lift the possible limitations due to the use of pseudocrystal wave functions. Two implementations of the PAW formalism, namely, the CP-PAW (Ref. 35) code and the Vienna *ab initio* simulation package (VASP) (Ref. 36) code, were applied, which also allow for the investigation of noncollinear spin orderings. The actual calculations were performed by employing a slab geometry where care was taken in using a well converged lateral k-point mesh (up to a 25×25 grid for the magnetic structures).

For the explicit many-body part of the modeling, an effective kinetic term associated with the realistic dispersion $\varepsilon_{\mathbf{k}}$ is combined with a Hubbard term, which incorporates the onsite Coulomb integral U, acting on a given lattice site i. Hence the resulting explicit interacting problem appears in the form of the Hubbard Hamiltonian, i.e.,

$$H=\sum_{\mathbf{k}\sigma}\varepsilon_{\mathbf{k}}d^{\dagger}_{\mathbf{k}\sigma}d_{\mathbf{k}\sigma}+U\sum_{i}n_{i\uparrow}n_{i\downarrow}, \tag{1}$$

where $\mathbf{k}$ denotes the crystal wave vector, $\sigma=\uparrow,\downarrow$ is the spin index, and $d^{(\dagger)}$ is the electron annihilation (creation) operator with $n_{i\sigma}=d^{\dagger}_{i\sigma}d_{i\sigma}$. It will be discussed in Sec. III A that indeed

a single-orbital form of the many-body description may be a reasonable first approximation for the present materials under consideration. The interacting problem posed by the Hamiltonian (1) was solved with two many-body techniques, namely, the DMFT with a Hirsch-Fye quantum Monte Carlo (QMC) impurity solver[37] and the rotationally invariant slave-boson (RISB) method[30,38] in saddle-point approximation. Note that in the single-site problem the RISB technique may also be understood as a quasiparticle impurity solution to DMFT. The employed mean-field version of the RISB method is in its character and nature of approximation very similar to the state-of-the-art Gutzwiller technique.[29,31,39]

The key interface between DFT and the many-body approaches at the present level of modeling is given by the representation of the LDA(-like) dispersion $\varepsilon_{\mathbf{k}}$ and the Hubbard U in Eq. (1). It asks for a suitable downfolding procedure of the original LDA problem to a local basis, i.e., the so-called correlated subspace (see, e.g., Refs. 40–42). The choice is in most cases a matter of convenience since many physically sound frameworks that provide a representation of the band structure within a minimal local Wannier(-type) basis are applicable. The coherent connection of the crystal problem to such a tailored basis is the key point, rather than the peculiarities of the (restricted) projected local viewpoint itself. It is important to realize that the extended (crystal, surface, or chain) problem, although composed of atoms, is *not* an atomic problem. Of course, in a subsequent many-body treatment the minimal interacting Hamiltonian has to be adjusted to the characteristics of the chosen local basis. Up to now, the results of such many-body approaches are not exceedingly sensitive to the very details of the selected correlated subspace, once the number and character of orbitals is agreed on. In that sense, the here utilized maximally localized Wannier (MLWF) scheme[43,44] thus provides a reliable local basis for the materials under consideration.

III. DFT INVESTIGATION AND MLWF DESCRIPTION

A. Single-site Sn unit cell

In order to investigate the electronic structure of the 1/3 monolayer of tin atoms on the semiconductor $\sqrt{3}\times\sqrt{3}R30°$ surfaces we first utilized slab geometries incorporating a single Sn atom within the full unit cell. Thus the surfaces are modeled by a supercell with three bilayers of (Si,Ge) separated by sufficiently large vacuum regions. Note that in this section we model the Sn submonolayer in each case as flat, although a distortion in z direction is observed for true Sn/Ge(111) (see Sec. III B). The Sn atoms are placed in the T_4 sites of the surface while the bottom of the slab is saturated with hydrogen atoms (see Fig. 1). Structural relaxations by minimizing the atomic forces have been performed with fixed position of the lowest substrate layer. The bulk chosen lattice constants and relaxed Sn-Sn nearest-neighbor distances are (5.43,6.65) Å and (5.65,6.93) Å for Sn/Si(111) and Sn/Ge(111), respectively. An energy cutoff of 16 Ry for the plane-wave part of the mixed-basis set was used for all calculations. Localized functions were introduced for Si($3s$,$3p$), Ge($3d$,$4s$,$4p$) as well as Sn($4d$,$5s$,$5p$). Note that hence the semicore d electrons of Ge and Sn are treated as valence in our computations and relativistic effects are included via the scalar-relativistic normconserving pseudopotentials. Since usually more appropriate for surface studies than LDA, we employed the GGA in the form of the Perdew-Burke-Ernzerhof (PBE) functional[45] to the exchange-correlation term in the density functional.

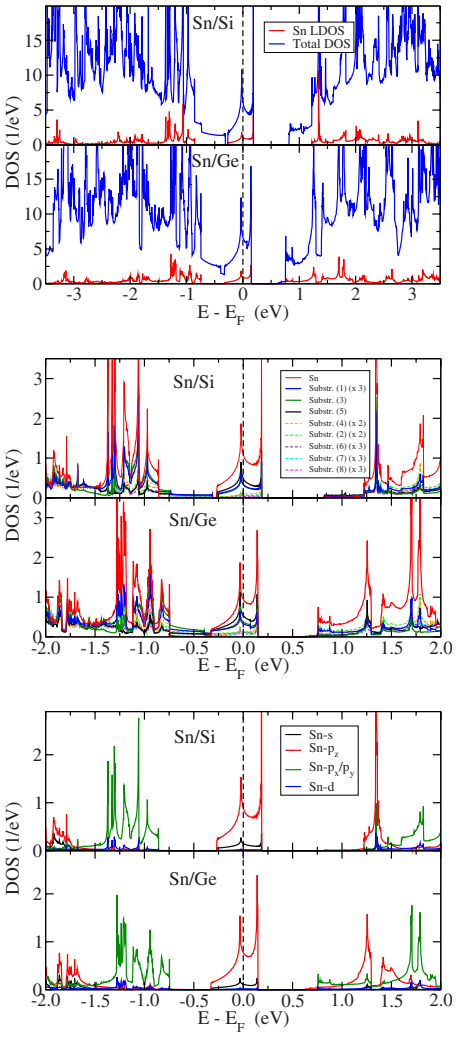

FIG. 2. (Color online) GGA-PBE DOS for Sn/(Si,Ge)(111) in the $\sqrt{3}\times\sqrt{3}R30°$ structure. (a) Total DOS together with local Sn DOS and (b) via contributions from different supercell atoms (for the labeling see Fig. 5). (c) Angular momentum resolved Sn DOS. Note that here the $5p_{x,y}$ curves are on top of each other.

The density of states (DOS) shown in Fig. 2 displays for both surface systems a prominent structure close to the Fermi level of width $W\sim 0.4$ eV [slightly larger for Sn/Ge(111)]. Two subpeaks are visible, one nearby the Fermi energy and the other at the upper energy edge in the unoccupied region. The major contributions to this low-energy part stems from the orbitals of the Sn adatom hybridizing with the orbitals of neighboring substrate atoms of the first and second layer [see Fig. 2(b)]. It becomes further obvious from the angular momentum resolved DOS in Fig. 2(c) that concerning the tin part the Sn($5p_z$) orbital is dominantly responsible for the low-energy weight. Minor contribution to this is also added by the Sn($5s$) orbital.

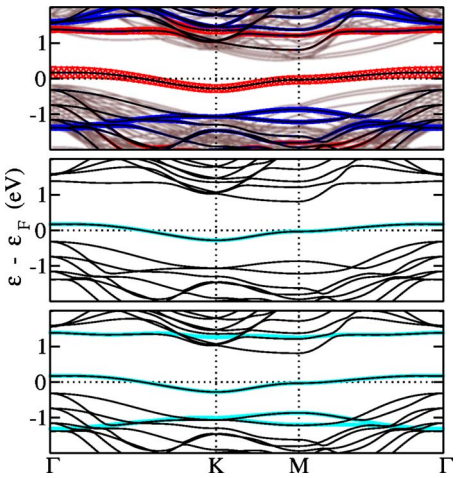

FIG. 3. (Color online) Top: surface band structure for the Sn/Si(111)-$\sqrt{3}\times\sqrt{3}R30°$ system, with fatbands for the Sn($5p$) orbitals (blue/gray: p_x, p_y; red/light gray: p_z). The bulk Si band structure is shown in the background. Middle: derived Wannier band (cyan/light gray) for the one-band model. Bottom: derived Wannier-type bands (cyan/light gray) for the four-band model.

As seen from the band-structure plots in Figs. 3 and 4, the low-energy DOS is associated with a single surface band within the gap of the bulk system. The so-called fatband resolution for the Sn($5p$) orbitals, i.e., the identification of the contribution of a given orbital character to a Kohn-Sham band at each k point via the width of a broadened coating "band," underlines the dominating p_z weight on this half-filled surface band. A straightforward MLWF construction may be applied to the single surface bands for both systems. The real-space Wannier function (see Fig. 5) shows not only the p_z-like lobe but displays additionally the threefold bonding aspects to the substrate atoms. A spread of 14.2 Å^2 for this MLWF was obtained in the case of Sn/Si(111). Albeit a rather similar low-energy state may be identified in the flat Sn/Ge(111) system, it has to be noted that conventional DFT has its problems in describing germanium systems. For the bulk material, there is a nearly vanishing band gap within

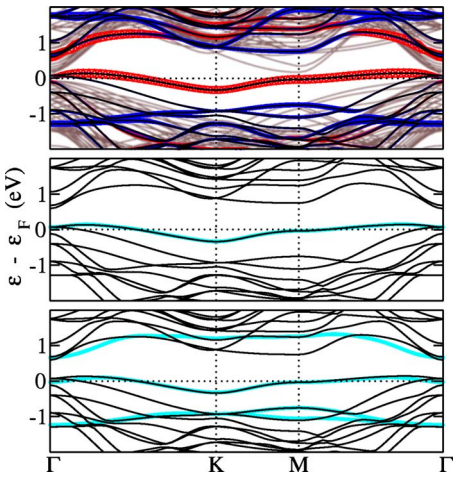

FIG. 4. (Color online) As Fig. 3 but here for the (flat) Sn/Ge(111)-$\sqrt{3}\times\sqrt{3}R30°$ system.

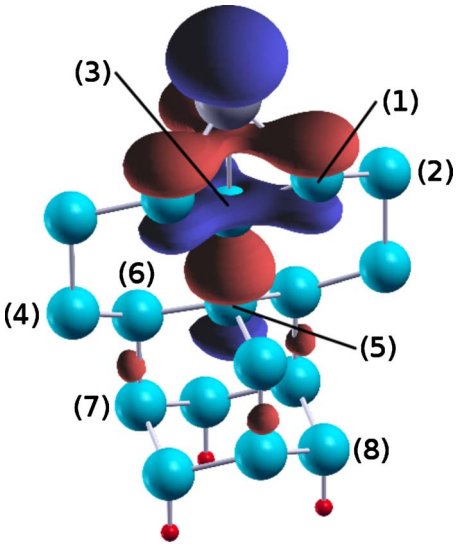

FIG. 5. (Color online) Wannier orbital corresponding to the one-band model. The numbers are references for the PBE-GGA DOS plot in Fig. 2.

DFT (Ref. 46) and additionally relativistic effects on the band structure are also important.[46,47] Still in our PBE-GGA study a single Wannier band may also be extracted in this case (see Fig. 4), however, contrary to Sn/Si(111) that band touches occupied levels at the Γ point.

Due to the substrate geometry and the apparent Sn($5s$) contribution at the Fermi level, an extended low-energy modeling based on sp^2-hybridized orbitals seems even more adequate for these systems. Indeed as shown in Figs. 3 and 4, the effective bands from the corresponding four-band MLWF construction fit well to the full Sn($5p$) fatband dispersion [Sn($5s$) has nearly exclusively weight on the band at the Fermi level]. The chemically more appealing sp^2+p_z viewpoint yields three of the four orbitals having a dominant in-plane orientation with an 120° angle between them while

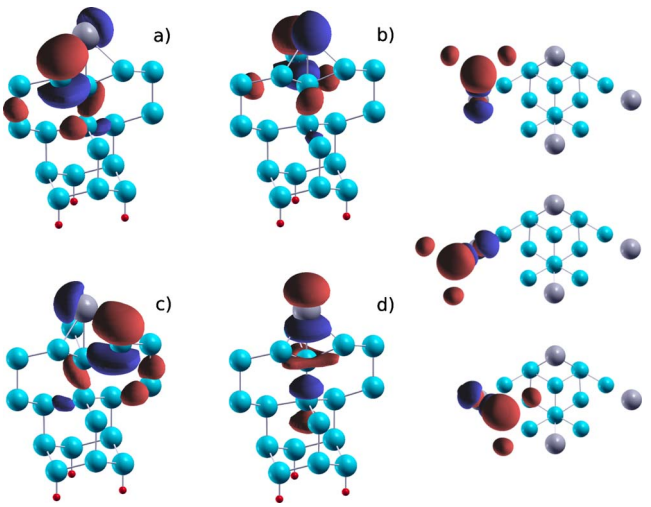

FIG. 6. (Color online) Left: Wannier-type orbitals of the four-band model. (a)–(c) sp^2-like orbitals and (d) p_z-like orbital. Right: top view on the spatial orientations of the three sp^2-like orbitals relative to the $\sqrt{3}\times\sqrt{3}R30°$ unit cell.

a fourth one is now directly reminiscent of the p_z orbital (see Fig. 6). This latter Wannier-type orbital has indeed major weight on the low-energy band close to ε_F. Compared to the one-band case, the spread of the Wannier-type functions are now given as 13.6 Å^2 for the sp^2-like orbitals and 20.8 Å^2 for the remaining p_z-like orbital.

The hopping integrals for both Wannier constructions are provided in Table I and Fig. 7. In the one-band model the nearest-neighbor hopping with an absolute value $|t| \sim 45$ meV is negative in accordance with the holelike dispersion from Figs. 3 and 4 around the Γ point. For the Sn/Ge(111) system the more distant hoppings are slightly larger whereas $|t|$ is somewhat smaller compared to the Sn/Si(111) case. The onsite energies in the four-band model yield a crystal-field splitting between the sp^2-like orbitals and the p_z-like one on the order of 1.6 (0.9) eV for Sn/(Si,Ge)(111). Though some caution has to be taken because of the named DFT-Ge problems, this illustrates the more isolated p_z-like level for the Si substrate and underlines the stronger hybridization in the case of the germanium substrate.

While the minimal one-band model is easily justified, the eligibility of the four-band model needs some additional comments. Albeit from the bonding character chemically meaningful, the orbital filling for this model amounts to five electrons in the present cases, i.e., one more than the half-filled sp valence of the carbon-group elements (Si, Ge, and Sn). Since equipped with similar electronegativity, a significant charge transfer in the strongly covalent surface systems is not expected. Still the five-electron filling may be acceptable as the Sn locality of the (sp^2+p_z)-like orbitals is neither very strong nor demanded on formal grounds. In addition we find this model more justified than a simpler three-band model for p-like orbitals only, which would in the end amount also to a five-electron filling for three effective

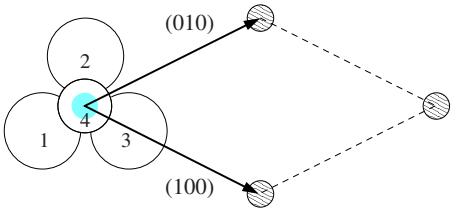

FIG. 7. (Color online) Illustration of the Wannier-type orbitals in the four-band model for the assignment of the hoppings in Table I. The sketched orbitals 1, 2, and 3 correspond to the top, middle, and bottom orbitals in the right part of Fig. 6. Orbital number 4 denotes the remaining p_z-like level.

TABLE I. Hopping integrals up to the fourth-nearest neighbors for the minimal one-band case (top) and the four-band (sp^2+p_z) model (bottom). For the latter 4×4 matrix, the column order is given (row order is identical), with the number in braces corresponding to the labeling in Fig. 7. Note that the values correspond to the entries of the real-space Wannier(-type) Hamiltonian, i.e., a minus sign is included.

Direction	100	110	200	210
Sn/Si(111)	44.6	−18.4	6.7	−0.8
Sn/Ge(111)	43.2	−23.7	7.3	−1.8

	Sn/Si hoppings (meV)				Sn/Ge hoppings (meV)			
Direction	$sp^2(1)$	$sp^2(2)$	$sp^2(3)$	$p_z(4)$	$sp^2(1)$	$sp^2(2)$	$sp^2(3)$	$p_z(4)$
000	−643.8	452.0	452.0	−318.6	−433.1	546.4	546.4	−358.3
	452.0	−643.8	452.0	−318.6	546.4	−433.1	546.4	−358.3
	452.0	452.0	−634.8	−318.6	546.4	546.4	−433.1	−358.3
	−318.6	−318.6	−318.6	990.3	−358.3	−358.3	−358.3	463.2
100	−42.6	−29.9	29.4	−26.7	−61.5	−37.8	3.6	−20.6
	−29.9	−42.6	29.4	−26.7	−37.8	−61.5	3.6	−20.6
	74.2	74.2	50.8	−33.1	33.8	33.8	2.9	70.9
	85.0	85.0	−49.1	16.7	54.9	54.9	1.6	29.2
110	−0.7	−5.9	−8.4	1.5	−15.2	−19.0	−22.8	1.3
	12.1	−9.5	−5.9	11.3	2.9	−22.8	−19.0	14.3
	3.8	12.1	−0.7	−24.5	−10.9	2.9	−15.2	−4.6
	−24.5	11.3	1.5	−9.4	−4.6	14.3	1.3	−10.3
200	−1.2	−1.4	4.2	−1.2	3.6	−4.2	2.8	3.6
	−1.4	−1.2	4.2	−1.2	−4.2	3.6	2.8	3.6
	−1.6	−1.6	8.0	1.9	−2.5	−2.5	0.6	7.3
	5.3	5.3	−2.8	−1.1	12.6	12.6	6.4	−10.5
210	0.7	0.3	0.9	−3.3	−4.3	−0.8	−2.5	0.8
	2.2	0.9	1.3	−0.5	−1.9	0.2	−2.7	−1.1
	−0.4	−2.9	0.0	−2.6	−2.4	−3.7	−0.9	−0.7
	0.0	−3.4	1.4	3.3	1.8	−3.0	1.5	2.9

bands. Such an extreme filling of 5/6 would render the interpretation in semilocal terms rather difficult, besides the inconsistency with the facts of the chemical bonding.

B. Three-site Sn unit cell

It is believed from experimental studies that the structural ground state of the Sn/Ge(111) system corresponds to a 2D-1U distortion of the Sn submonolayer.[9] To be able to account for this reconstruction (cf. Fig. 1), we thus performed electronic-structure calculations using a 3×3 supercell with a difference $\Delta=0.32$ Å between the up-down Sn positions,[16] which we applied to our PBE-GGA structurally relaxed unit cell with the planar submonolayer. In these extended supercell calculations only one orbital per Sn adatom is included in the subsequent MLWF construction. This results in a Kohn-Sham-Wannier Hamiltonian which corresponds to a single-orbital problem on a three-site triangular cluster. For comparison, we derived such enlarged Hamiltonians also for the flat systems via corresponding larger unit-cell calculations for planar Sn/(Si,Ge)(111). The resulting Wannier-type bands are shown in Fig. 8. The bands again fit exactly in the Sn/Si(111) case, whereas for the distorted Sn/Ge(111) surface a shift toward lower lying bands at the Γ point is visible. The latter feature is again due to the band hybridizations already observed in the single-site Sn unit cell. It may be observed that the 2D-1U surface reconstruction leads to a small splitting of the low-energy bands, affecting mainly the occupied part of these states.

Besides the study of the influence of apparent surface reconstructions, the investigation of the magnetic behavior seems a most important endeavor. As already outlined in Sec. I, the quasi-2D triangular Sn submonolayer might be a realistic case for the application of model ideas discussed in the context of 2D quantum magnetism. For instance, it is strongly suspected that the half-filled Hubbard model on the triangular lattice in the large-U limit displays a 120° noncollinear spin ordering (e.g., Ref. 48). Thus if in the present triangular system nearest-neighbor AFM exchange is at work, the latter pattern is among the candidates for an ordered phase (even in the metallic regime). Therefore we investigated possible magnetic orderings within PBE-GGA, especially for the Sn/Si(111) system where intricate ordering patterns are heavily discussed.[4,20] Although (finite-temperature) magnetism would be very interesting, one has to keep in mind that the constituents (Sn, Si, and Ge) are no high-susceptible magnetic materials. The sp bonding (involving large principal quantum numbers) with filled d states renders magnetism from a chemical point of view questionable. Furthermore the rather large Sn-Sn nearest-neighbor distance of ~6.7 Å, asks for a robust exchange path to facilitate the appearance of long-range order. Still the low-dimensional 2D character might be sufficient to induce delicate magnetic behavior. Note also that the high DOS close to the Fermi level (cf. Fig. 2) might give rise to flat-band ferromagnetism.[49,50]

The results of our investigation of different magnetic orderings on planar Sn/Si(111) 3×3 are summarized in Table II. The calculations show that especially the ferromagnetic (FM) order is rather intriguing. One may stabilize a FM solution for Sn/Si(111), resembling previous work by Profetta and Tosatti,[20] however, this state is energetically unfavorable compared to the nonmagnetic (NM) solution. The corresponding local energy minimum of this FM state appears to be rather flat, thus already small disturbances drive the DFT self-consistency cycle toward the NM state. This was confirmed within all three utilized band-structure codes, i.e., MBPP, CP-PAW, and VASP, whereby the Sn-substrate distance does not influence this qualitative result. Note the rather small local M_{Sn} moment compared to total FM moment of the supercell. Thus this metastable FM state is far from being originated from pure local Sn moments but has significant nonlocal character. Since collinear AFM order is impossible due to frustration on the undistorted lattice, a collinear ferrimagnetic ordering (two up spins and one down spin on the minimal triangle) as well as the in-plane noncollinear 120° state were investigated. Indeed, both latter ordering patterns are found to be stable with respect to the nonmagnetic solution, with the lowest total energy for the 120° ordering. Though the local Sn magnetic moments M_{Sn} are only on the order of $\sim0.06\mu_{\mathrm{B}}$ within PBE-GGA, detailed convergence studies elucidated nonetheless their nonzero value. Note that these local M_{Sn} are supplemented by additional spin polarization on the remaining sites and the interstitial contribute. Hence again the picture of strictly localized magnetism is not appropriate on the weakly correlated modeling level but still local moments with small AFM exchange may exist in these Sn submonolayers. Those may possibly give rise to spin-liquid physics or eventual magnetic long-range order also in the correlated regime.[13]

Similar magnetic PBE-GGA studies for a model *planar* Sn/Ge(111) 3×3 surface did not result in magnetic long-range order. The stronger hybridization of the Ge($4s4p$) states with tin should generally weaken the magnetic tendencies compared to the silicon substrate. We did not investigate the more realistic 2D-1U reconstructed structure in this matter, which is left for further studies.

IV. INVESTIGATION OF ELECTRONIC CORRELATIONS

In order to take the principal effect of electronic correlations into account, we concentrate in the following on the realistic one-band models derived in Sec. III A and their cluster extension from Sec. III B. Furthermore we restrict the investigations to paramagnetic modelings, i.e., do not cover possible magnetic orderings. Since it became clear from Sec. III B that the energy scale for magnetic long-range order is rather small, such an analysis shall be postponed to future studies.

A. LDA+DMFT(QMC) study

By combining our Wannier Hamiltonians with the DMFT framework we are in the position to reveal the spectral function of the surface systems in the interacting regime. Due to the small bandwidth of $W\sim0.4$ eV, already small absolute values for the Hubbard U may introduce strong correlation effects. Although the low-energy bands of the discussed sys-

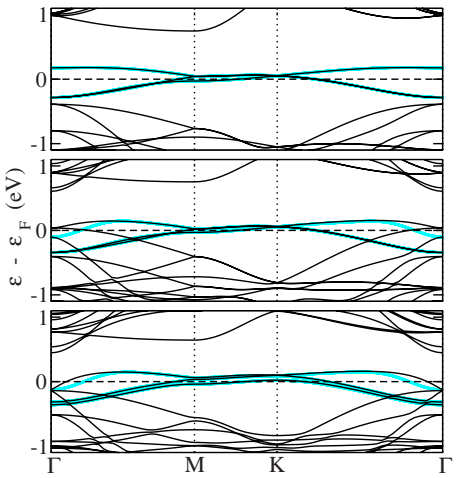

FIG. 8. (Color online) PBE-GGA band structure (dark) with extracted Wannier(-type) bands (cyan/gray) for the 3×3 supercell. Top: planar Sn/Si(111) system. Middle: planar Sn/Ge(111) system. Bottom: Sn/Ge(111) with the 2D-1U reconstruction.

tems are mainly composed of Sn($5s,5p$) states, an onsite Coulomb interaction of this order of magnitude may very well be reasonable. In general, the Hubbard U of course depends on the choice of the orbital basis set. Since we are here working with the low-energy one-band model, the actual U should be different from the one in a larger multi-site basis. In metallic bulk systems, the latter usually involves more localized orbitals than a small onsite orbital basis and hence leads to a comparatively larger U (to be further screened within the larger basis). However, since here the semiconducting substrate is involved, the screening effects perpendicular to the surface are weaker. Also we are still working in an onsite basis. Thus, and also because of the supercell architecture, the effective p_z-like Wannier orbital in the four-band model is therefore not very well localized.

The results of the paramagnetic single-site DMFT(QMC) calculations for the realistic one-band model are displayed in Fig. 9 for different choices of the Hubbard U. Of course, due to the simplicity of the modeling the spectral function (finally obtained via the maximum-entropy method) follows the usual behavior with increasing U, i.e., a low-energy band narrowing with the additional appearance of Hubbard-band features at higher energies takes place. The Mott transition is

TABLE II. Comparison of the different magnetic orderings in the flat Sn submonolayer of the $\sqrt{3}\times\sqrt{3}R30°$ surface with the Si substrate. The energies E and total moments M are given with respect to the nonmagnetic structure in PBE-GGA and correspond to an enlarged 3×3 unit cell. This cell incorporates 66 atoms, namely, 54 Si, 3 Sn, and 9 H atoms (for saturation of the bottom bulklike Si layer).

Magnetic ordering	E (meV)	M (μ_B)	M_{Sn} (μ_B)
Ferromagnetic	1.5	0.80	0.031
Collinear ferrimagnetic	−1.6	0.44	0.055
120° noncollinear	−3.6	0.00	0.058

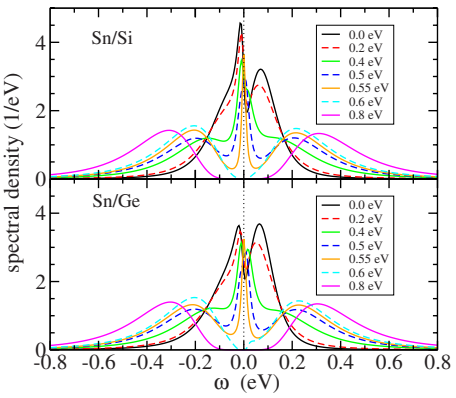

FIG. 9. (Color online) Realistic single-site DMFT(QMC) results for the planar one-band models at $\beta=200$ eV^{-1} ($T\sim58$ K).

reached at a critical value of about $U_c\sim0.6$ eV for the Sn/Si(111) surface systems [with a somewhat larger value for planar Sn/Ge(111)]. Since this transition shows a weak first-order character in the calculations (see also Sec. IV B) critical interactions U_{c1}, U_{c2} govern this regime, respectively. However, in the present study, due to the simplicity of the one-band modeling, we did not map out the respective hysteresis loops. The energy gap within the insulating Mott state is on the order of ~0.2 eV for $U\sim0.7$ eV with Hubbard bands at around 0.3 eV above and below E_F for both Sn/(Si,Ge)(111) systems. The position of our Hubbard excitations is roughly in line with the region of increased spectral-weight transfer measured in photoemission experiments[4,6] below 30K. Hence a rather small Hubbard U, slightly larger than the single bandwidth, is sufficient to drive the Sn-dominated surface band Mott insulating. This value is, however, not very surprising since from the involved quantum numbers of the respective states no large value of U (i.e., as for transition-metal and/or f systems) is expected.

In order to study the importance of intersite self-energy effects, especially for the distorted Sn/Ge(111) case, we also performed cluster DMFT (CDMFT) (for recent reviews see, e.g., Refs. 51–53) computations within the cellular cluster framework for the basic Sn triangle in the submonolayer. The resulting spectral functions are shown in Fig. 10. Note that we employed a somewhat higher temperature within the QMC solver because of the larger numerical effort in the cluster framework. For the planar Sn/Si(111) case the main differences to the single-site results are given by a slightly smaller $U_c\sim0.55$ eV, smaller energy gap and Hubbard bands in some closer range to the low-energy region. We checked that those observations are not only due to the different temperatures of our computations. One may also observe a stronger asymmetry in the spectrum up and below the Fermi level, with some stronger reduction in low-energy spectral weight below E_F. For the site-resolved spectral function of the Sn/Ge(111) 3×3 system in the distorted 2D-1U structure it is first important to remark that the two downward-shifted Sn atoms are inequivalent by symmetry due to different hybridization with the "up" atom even assuming the same height for the "down" 2D atoms[19,54] (see Sec. III B). The latter are moreover less occupied than the upward-shifted Sn atom.[8] With increasing U, this filling im-

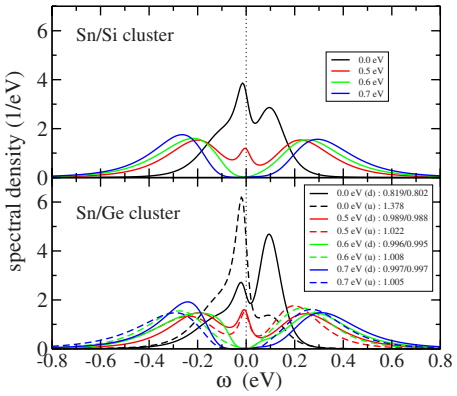

FIG. 10. (Color online) Realistic cellular-cluster DMFT(QMC) results for planar Sn/Si(111) and 2D-1U Sn/Ge(111). The up/down tags refer to the inequivalent atomic positions and the numbers yield the orbital occupation. Note that albeit slightly different by symmetry, we only show the averaged spectral function for the two-down atoms (occupations are site selective though). Calculations were performed at $\beta=70$ eV^{-1} ($T\sim 166$ K).

balance because of the distortion-induced crystal-field shifts becomes smaller and is compensated at the Mott transition (see Fig. 10). However, a slightly larger critical U_c compared to the planar cluster for Sn/Ge(111) is necessary to reach this transition (more or less equivalent to the critical U within the planar single-site DMFT). The above-noted spectral asymmetry in the occupied and unoccupied part is even larger in the distorted case.

B. LDA+RISB study

In addition to DMFT(QMC) computations we have performed slave-boson calculations within the RISB framework to further verify our results and to achieve a better resolution of the qualitative differences in values for the critical U in the various cases. Furthermore we also want to elucidate the intersite spin correlations in the cellular cluster modeling. The RISB results for the quasiparticle weight Z are shown in Fig. 11. In the one-band case, the RISB method yields for both flat systems a first-order transition from the paramagnetic metal to the paramagnetic insulator. The corresponding critical U values are given by $U_c\sim 0.75$ eV (0.78 eV) for Sn/(Si,Ge)(111) $\sqrt{3}\times\sqrt{3}R30°$, hence show the same qualitative trend as DMFT(QMC). A somewhat larger absolute value within RISB is understandable from the saddle-point approximation which is identical to the neglection of quantum fluctuations. The cellular-cluster investigations again verify the reduced critical Hubbard U values [similar to the ones from DMFT(QMC)] due to an increase in the correlation strength via the inclusion of the nearest-neighbor self-energies. Also the enhanced U_c for the distorted 2D-1U structure of Sn/Ge(111) is a solid result. Note that the first-order character of the transition is strengthened in the cluster modeling. For a commensurable Mott transition the correlations have to drive additional charge transfers between the Sn site in the 2D-1U structure. The therefore enhanced charge fluctuations in the latter case may thus account for the larger U_c.[15] In Fig. 12 we show the continuous development of the individual site fillings with increasing U for the 2D-1U structure. The corresponding labeling of the different Sn atoms is given in the inset of Fig. 12. As it is clearly seen, the originally enhanced occupation of the low-energy orbital for the upward-shifted Sn atom on the cluster becomes reduced with increasing U while the downward-shifted ones gain electron filling in their respective orbitals. This is in line with the results obtained from the more elaborate QMC solver to DMFT (cf. Fig. 10).

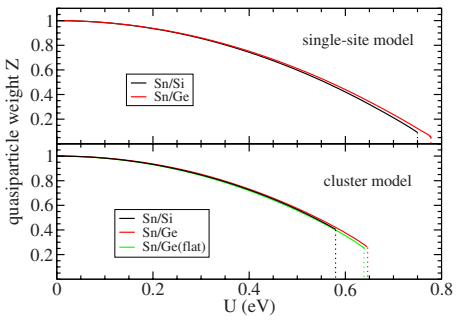

FIG. 11. (Color online) RISB results for the quasiparticle weight Z for the planar single-site (top) and the cellular-cluster (bottom) models.

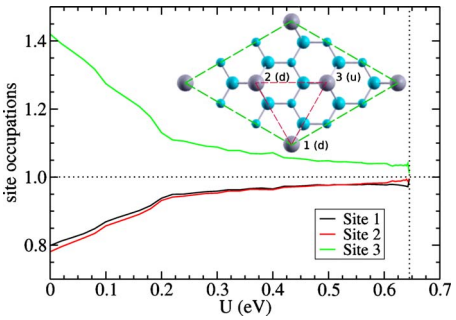

FIG. 12. (Color online) Orbital occupations of the different Sn atoms in the 2D-1U structure for Sn/Ge(111) obtained from the cellular cluster calculation with varying U. Inset: designation of the different Sn atoms in the cellular cluster description of Sn/Ge(111) from a top view on the surface. The (red/gray) dashed lines mark the cluster utilized for the cellular modeling.

To provide some insight into the magnetic behavior with taking into account electronic correlations, Fig. 13 displays the local spin correlations $\langle \mathbf{S}_i\cdot\mathbf{S}_j\rangle$ between the Sn atoms from the low-energy modeling. It is seen that the spin correlations are always negative, i.e., of AFM character, as expected by considering the superexchange induced via U. Naturally, the degree of magnetic behavior is therewith increased compared to the noninteracting case. The comparison of the two different substrates with the planar geometry of the Sn submonolayer exhibits the stronger magnetic correlations within the Sn/Si(111) system. Thus the qualitative result obtained from the weakly correlated PBE-GGA modeling extends to the strongly correlated treatment. In the 2D-1U structure of Sn/Ge(111), the values of $\langle \mathbf{S}_i\cdot\mathbf{S}_j\rangle$ for the now different Sn-Sn pairs show interesting behavior. Somewhat counterintuitive, the spin correlations between the two up-down pairs, here denoted Sn(1)-Sn(3) and Sn(2)-Sn(3), scale rather differently with increasing U. While for the Sn(2)-Sn(3) pair $\langle \mathbf{S}_i\cdot\mathbf{S}_j\rangle$ is

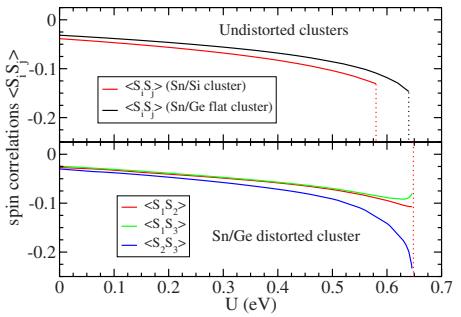

FIG. 13. (Color online) Spin-correlation functions for the Sn/Si(111) and the Sn/Ge(111) distorted cluster obtained from the RISB study. Top: planar systems, bottom: distorted 2D-1U Sn/Ge(111) system. The vertical line marks the critical U value, respectively.

most negative, for the Sn(1)-Sn(3) pair the spin correlations become nonmonotonic close to U_c, anticipating tendencies to eventual FM coupling. The remaining Sn(1)-Sn(2) pair of the two-down atoms scales in between these functions. This result can be explained by the fact that the absolute value of the hopping amplitude t is maximum between the Sn(2)-Sn(3) pair and is accordingly weakened between Sn(1)-Sn(3). Because of the upward shift of the Sn(3) atom, the lobe from its effective Wannier orbital pointing toward Sn(2) achieves a wider range, leading to stronger overlap with the Wannier orbital of Sn(2).

In order to touch base with the DFT results in Sec. III B on the magnetic behavior, we also extracted the effective onsite spin quantum number S and the average angle α between the effective spins on the triangular cluster from the cellular-cluster RISB calculation for the Sn/Si(111) system (cf. Fig. 14). While $|\mathbf{S}_i|=\sqrt{\mathbf{S}_i^2}=S(S+1)$, the angle α may be computed from $\langle \mathbf{S}_i \cdot \mathbf{S}_j \rangle = \langle |\mathbf{S_i}||\mathbf{S_j}| \cos\alpha \rangle$. As expected and in line with the DFT result, for small U the spin quantum number S is far away from the local-electron-spin value $S=1/2$ because of the strongly itinerant regime. However, with increasing U this limiting value is approached but still not reached close to the critical U_c. Because of the considerable first-order character of the metal-insulator transition in the cellular-cluster scheme, this is not in contradiction to the nearby onset of the insulating Mott state. The average α asks for a more subtle discussion. Since the calculation was performed in the PM state, $\langle \mathbf{S}_i \rangle = 0$ holds on every site, i.e., no spatial direction is locally preferred. The limiting collinear cases are the trivial FM one (average $\alpha=0$) and the case when one local spin shows AFM coupling to the remaining two FM coupled spins (average $\alpha=120°$). The latter frustrated case is of course completely different from a true 120° noncollinear spin ordering. From the resulting average α in the PM phase displayed in Fig. 14 one can only read off that the AFM correlations between the spins are truly enhanced on the triangular cluster for increasing U. But the possible 120° noncollinear phase may not be directly reachable from the PM metallic phase. Note that in model studies (e.g., Ref. 48) the former ordering only appears far in the insulating phase, when the system is somewhat close to the Heisenberg limit. Of course, this result does not rule out the possibility that due to the specific electronic characteristics of the present realistic system, the 120° noncollinear ordering shows up earlier and even already in the metallic phase, as motivated by the DFT results. However, in order to investigate this from an interacting many-body picture, one would have to try to stabilize that ordered phase for finite U and, as within the DFT calculations, taking also the substrate-induced anisotropies into account.

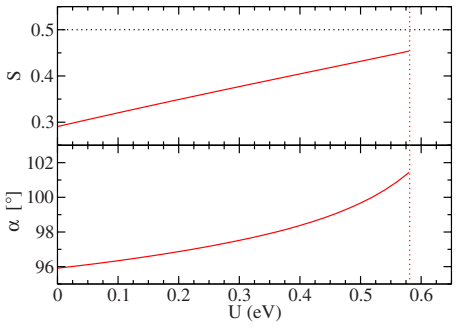

FIG. 14. (Color online) Interaction-dependent spin quantum number S (top) and average angle α between the spins on the basic triangular cluster (bottom) for the case of the Sn/Si(111) system.

V. SUMMARY

We have presented a detailed modeling of the Sn/(Si,Ge)(111) surface systems using state-of-the-art band-structure methods combined with many-body techniques. In addition to previous DFT investigations we extracted realistic one- and four-band Wannier(-type) Hamiltonians that are capable of describing the electronic structure close to the Fermi level. The physics of the minimal one-band model is of course restricted, however, due to the prominent Sn-dominated half-filled surface band at ε_F, especially for Sn/Si(111) $\sqrt{3}\times\sqrt{3}R30°$ this is believed to be an adequate modeling viewpoint. The atomistic description of the Sn/Ge(111) system still raises some questions concerning the apparent limitations of simplified exchange-correlation functionals in this case. Nonetheless on the present level of investigation and comparison, the PBE-GGA perspective appears sufficient to reveal the essential differences between both surface systems. The hybridization of the Sn submonolayer with the substrate is stronger in the case of Ge, leading there to a more intriguing entanglement of that layer with the supporting atoms below. Consequently, structural reconstructions are more likely and indeed take place as verified in experimental studies.

The magnetic behavior in these systems renders them most fascinating from a fundamental physics point of view in terms of possible low-dimensional quantum magnetism. The (non)collinear spin-polarized DFT calculations revealed that there is indeed the chance for intricate magnetic orderings. In this respect we found the 120°-noncollinear structure to be the magnetic ground state in the weakly correlated description. Further theoretical studies, including the effect of true many-body correlations on the magnetism are important and should be motivated by the present work. Although the resulting moments are rather small, maybe advanced experi-

mental techniques are capable of exploring these small energy scales.

Using DMFT(QMC) and RISB techniques, a moderate value on the order of $U \sim 0.5-0.6$ eV was found to govern the systems from a one-band Hubbard-type model in a strongly correlated limit. Because of the small low-energy bandwidth it is reasonable to expect electronic correlations to be important, however, sole local Coulomb interactions are surely limited in the description of these systems based on carbon-group elements. Yet already on this rather simple level a delicate interplay between the structural and electronic degrees of freedom, anticipated in other model(-like) frameworks,[13,15] was verified on the grounds of an LDA +DMFT approach. Future studies now have to concentrate on including the substrate degrees of freedom explicitly in the modeling of the interacting electronic structure, perhaps even allowing for the dynamical structural reconstructions needed for Sn/Ge(111).

ACKNOWLEDGMENTS

We thank C. Piefke, L. Boehnke, J. Wiebe, and S. Modesti for helpful discussions. Financial support was provided by the SFB668 and the NANOSPINTRONICS Cluster of Excellence. Computations were performed at the Linux-Cluster of the RRZ at the University of Hamburg as well as the North-German Supercomputing Alliance (HRLN).

[1] J. M. Carpinelli, H. H. Weitering, E. W. Plummer, and R. Stumpf, Nature (London) **381**, 398 (1996).
[2] H. H. Weitering, X. Shi, P. D. Johnson, J. Chen, N. J. DiNardo, and K. Kempa, Phys. Rev. Lett. **78**, 1331 (1997).
[3] T. Zhang *et al.*, Nat. Phys. **6**, 104 (2010).
[4] S. Modesti, L. Petaccia, G. Ceballos, I. Vobornik, G. Panaccione, G. Rossi, L. Ottaviano, R. Larciprete, S. Lizzit, and A. Goldoni, Phys. Rev. Lett. **98**, 126401 (2007).
[5] H. Morikawa, I. Matsuda, and S. Hasegawa, Phys. Rev. B **65**, 201308 (2002).
[6] R. I. G. Uhrberg, H. M. Zhang, T. Balasubramanian, S. T. Jemander, N. Lin, and G. V. Hansson, Phys. Rev. B **62**, 8082 (2000).
[7] A. Charrier, R. Pérez, F. Thibaudau, J.-M. Debever, J. Ortega, F. Flores, and J.-M. Themlin, Phys. Rev. B **64**, 115407 (2001).
[8] J. Avila, A. Mascaraque, E. G. Michel, M. C. Asensio, G. LeLay, J. Ortega, R. Pérez, and F. Flores, Phys. Rev. Lett. **82**, 442 (1999).
[9] O. Pulci, M. Marsili, P. Gori, M. Palummo, A. Cricenti, F. Bechstedt, and R. del Sole, Appl. Phys. A **85**, 361 (2006).
[10] R. Cortés, A. Tejeda, J. Lobo, C. Didiot, B. Kierren, D. Malterre, E. G. Michel, and A. Mascaraque, Phys. Rev. Lett. **96**, 126103 (2006).
[11] S. Colonna, F. Ronci, A. Cricenti, and G. LeLay, Phys. Rev. Lett. **101**, 186102 (2008).
[12] H. Morikawa, S. Jeong, and H. W. Yeom, Phys. Rev. B **78**, 245307 (2008).
[13] G. Santoro, S. Scandolo, and E. Tosatti, Phys. Rev. B **59**, 1891 (1999).
[14] G. Profeta, A. Continenza, L. Ottaviano, W. Mannstadt, and A. J. Freeman, Phys. Rev. B **62**, 1556 (2000).
[15] F. Flores, J. Ortega, R. Pérez, A. Charrier, F. Thibaudau, J.-M. Debever, and J.-M. Themlin, Prog. Surf. Sci. **67**, 299 (2001).
[16] S. de Gironcoli, S. Scandolo, G. Ballabio, G. Santoro, and E. Tosatti, Surf. Sci. **454-456**, 172 (2000).
[17] R. Pérez, J. Ortega, and F. Flores, Phys. Rev. Lett. **86**, 4891 (2001).
[18] G. Ballabio, G. Profeta, S. de Gironcoli, S. Scandolo, G. E. Santoro, and E. Tosatti, Phys. Rev. Lett. **89**, 126803 (2002).
[19] P. Gori, F. Ronci, S. Colonna, A. Cricenti, O. Pulci, and G. LeLay, EPL **85**, 66001 (2009).
[20] G. Profeta and E. Tosatti, Phys. Rev. Lett. **98**, 086401 (2007).
[21] V. I. Anisimov, J. Zaanen, and O. K. Andersen, Phys. Rev. B **44**, 943 (1991).
[22] V. I. Anisimov, A. I. Poteryaev, M. A. Korotin, A. O. Anokhin, and G. Kotliar, J. Phys.: Condens. Matter **9**, 7359 (1997).
[23] A. I. Lichtenstein and M. I. Katsnelson, Phys. Rev. B **57**, 6884 (1998).
[24] A. Georges and G. Kotliar, Phys. Rev. B **45**, 6479 (1992).
[25] W. Metzner and D. Vollhardt, Phys. Rev. Lett. **62**, 324 (1989).
[26] J. Bünemann *et al.*, Europhys. Lett. **61**, 667 (2003).
[27] X. Y. Deng, X. Dai, and Z. Fang, EPL **83**, 37008 (2008).
[28] F. Lechermann, Phys. Rev. Lett. **102**, 046403 (2009).
[29] J. Bünemann, W. Weber, and F. Gebhard, Phys. Rev. B **57**, 6896 (1998).
[30] F. Lechermann, A. Georges, G. Kotliar, and O. Parcollet, Phys. Rev. B **76**, 155102 (2007).
[31] M. Fabrizio, Phys. Rev. B **76**, 165110 (2007).
[32] B. Meyer, C. Elsässer, F. Lechermann, and M. Fähnle, FORTRAN 90 *Program for Mixed-Basis-Pseudopotential Calculations for Crystals*, Max-Planck-Institut für Metallforschung, Stuttgart (unpublished).
[33] S. G. Louie, K. M. Ho, and M. L. Cohen, Phys. Rev. B **19**, 1774 (1979).
[34] D. Vanderbilt, Phys. Rev. B **32**, 8412 (1985).
[35] P. E. Blöchl, Phys. Rev. B **50**, 17953 (1994).
[36] G. Kresse and J. Hafner, J. Phys.: Condens. Matter **6**, 8245 (1994).
[37] J. E. Hirsch and R. M. Fye, Phys. Rev. Lett. **56**, 2521 (1986).
[38] T. Li, P. Wölfle, and P. J. Hirschfeld, Phys. Rev. B **40**, 6817 (1989).
[39] J. Bünemann and F. Gebhard, Phys. Rev. B **76**, 193104 (2007).
[40] F. Lechermann, A. Georges, A. Poteryaev, S. Biermann, M. Posternak, A. Yamasaki, and O. K. Andersen, Phys. Rev. B **74**, 125120 (2006).
[41] G. Kotliar, S. Y. Savrasov, K. Haule, V. S. Oudovenko, O. Parcollet, and C. A. Marianetti, Rev. Mod. Phys. **78**, 865 (2006).
[42] V. I. Anisimov *et al.*, Phys. Rev. B **71**, 125119 (2005).
[43] N. Marzari and D. Vanderbilt, Phys. Rev. B **56**, 12847 (1997).
[44] I. Souza, N. Marzari, and D. Vanderbilt, Phys. Rev. B **65**, 035109 (2001).
[45] J. P. Perdew, K. Burke, and M. Ernzerhof, Phys. Rev. Lett. **77**,

3865 (1996).
[46] G. B. Bachelet and N. E. Christensen, Phys. Rev. B **31**, 879 (1985).
[47] D. Glötzel, B. Segall, and O. K. Andersen, Solid State Commun. **36**, 403 (1980).
[48] T. Yoshioka, A. Koga, and N. Kawakami, Phys. Rev. Lett. **103**, 036401 (2009).
[49] A. Mielke, J. Phys. A **24**, L73 (1991).
[50] H. Tasaki, Phys. Rev. Lett. **69**, 1608 (1992).
[51] A. Lichtenstein, M. Katsnelson, and G. Kotliar, *Electron Correlations and Materials Properties 2* (Kluwer Academic, New York, 2003).
[52] G. Biroli, O. Parcollet, and G. Kotliar, Phys. Rev. B **69**, 205108 (2004).
[53] T. Maier, M. Jarrell, T. Pruschke, and M. H. Hettler, Rev. Mod. Phys. **77**, 1027 (2005).
[54] A. Tejeda, R. Cortés, J. Lobo-Checa, C. Didiot, B. Kierren, D. Malterre, E. G. Michel, and A. Mascaraque, Phys. Rev. Lett. **100**, 026103 (2008).